13th International Brick and
Block Masonry Conference
Amsterdam, July 4-7, 2004

3-D FINITE ELEMENT MODELLING OF MASONRY-INFILLED FRAMES WITH AND WITHOUT OPENINGS

Wael W. El-Dakhakhni[1] and Robert G. Drysdale[2]

Abstract

Masonry infill walls in frame structures have been long known to affect strength, stiffness, and ductility of the composite structure. In seismic areas, ignoring the composite action is not always on the safe side, since the interaction between the wall and the frame under lateral loads dramatically changes the stiffness and the dynamic characteristics of the composite structure, and hence, its response to seismic loads. This paper presents a parametric study on the effects of openings on the stiffness, internal load distribution and strength of the composite structure using 3-D finite element modelling. The finite element models were compared against experimental results obtained by others and showed good agreement. The modelling technique serves as a basis for providing improved understanding in the local and global behaviour of masonry-infilled frame structures.

Key Words

3-D Models; Concrete masonry; Finite element method; Infill walls; In-plane; Seismic load; Shear; Structural frames; Openings.

1 Introduction

Masonry infill panels can be found as interior and exterior walls in reinforced concrete and steel frame structures. In recent years they have been considered to serve as partition walls and part of the exterior building envelope. Being considered as architectural elements, their presence is often ignored by structural engineers. However, unless they are separated from the frames by adequate movement joints along the ends and top, they will interact with the surrounding frame when the structure is subjected to wind or earthquake loads; the resulting system is referred to as an *infilled frame*.

Ignoring the effect of the infill in designing new buildings or in analysing existing ones for upgrading purposes is not always conservative. It depends on the site where the

[1] Post-doctoral fellow, McMaster University Centre for Effective Design of Structures, Hamilton, ON, Canada. E-mail: eldak@mcmaster.ca
[2] Martini, Mascarin and George Chair in Masonry Design and Director of McMaster University Centre for Effective Design of Structures, Hamilton, ON, Canada. E-mail: drysdale@mcmaster.ca

building is located in order to decide whether the inclusion or exclusion of infill walls is conservative or not. This effect is shown in Fig. 1, where T_{if} is the fundamental period of vibration for the infilled frame structure, and T_{bf} is the fundamental period of vibration for the bare frame structure. For an earthquake having a response spectrum following Curve A, the spectral acceleration and consequently the base shear attracted by the structure increases as a result of including the infill. Alternatively, for an earthquake having a response spectrum following Curve B, the base shear attracted by the structure would decrease when the infill is included [Comite (1996)].

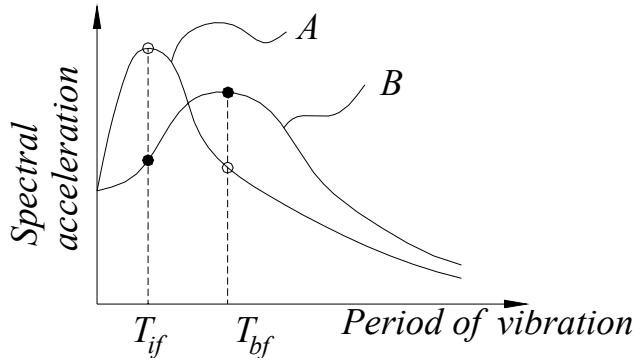

Figure 1 Possible Effects of the Infill Walls Depending on Different Earthquake Response Spectra

The paper presents a parametric study using 3-D FE analysis of the different effects of masonry strength, boundary conditions and opening sizes and shapes on the stiffness, strength, possible struts mechanisms and failure modes within the wall or the surrounding frame. In order to verify the model, the predicted results were compared to data from an experimental study reported by El-Dakhakhni et al. (2004). In their study, El-Dakhakhni et al. (2004) evaluated the behaviour of different masonry infilled frames under displacement controlled cyclic loading. All the frames were identically made of W10x22 steel sections with moment resisting connections. The 2.8 m high by 3.4 m long walls were built on a 19 mm base steel plate connecting also the two column bases which were anchored to the structural floor using two 62 mm bolts. The walls were built using standard 15 cm hollow concrete block with Type S mortar applied on the face shells.

2 Modelling Infilled Frame Behaviour

Modelling concrete masonry infilled steel frames is complicated due to: nonlinearity of the masonry material, the existence of the mortar joint planes of weakness, the masonry block geometry, cracking and crushing of the infill wall, nonlinear frame behaviour and relative movement along the frame-wall interface. This latter effect is a highly nonlinear contact problem existing because of the typical construction practice of not creating any positive connection between the infill wall and the surrounding frame. Factors affecting the contact behaviour include: coefficient of friction, cohesion, maximum shear stress developed at the interface and normal and shear contact stiffnesses. In addition, the full Newton-Raphson solution method required for contact problem solving within the ANSYS finite element (FE) [ANSYS (2002)-a] code used in this study requires considerable computation time.

In addition to the above difficulties, the accurate representation of all the geometric features of the frame and the infill wall is paramount to obtain a model that can simulate the behaviour of the actual structure. After verifying the validity of the modelling approach, a parametric study can be conducted to evaluate the effect of different parameters on the infilled frame structure behaviour. This can include

modelling other untested parameters (virtual specimens) without the need to carry out the more expensive and time consuming experimental research.

3 Modelling Assumptions

The Drucker-Prager failure criterion [ANSYS (2002)-a] was utilized to model the masonry wall material. This criterion has a yield surface that does not change with progressive yielding. Hence there is no hardening rule and the material is elastic-perfectly plastic. The criterion is a modification of the Von Mises yield criterion to account for the influence of the hydrostatic pressure component; the higher the confinement pressure the higher the failure strength. ANSYS eight node solid elements, SOLID45 [ANSYS (2002)-b] were used to model the wall and four node plastic shell elements, SHELL143 [ANSYS (2002)-b] were employed to model the steel frame members with both membrane and flexure behaviour enabled. The contact algorithm chosen to represent the contact between the masonry wall face shell and the steel column and beam flanges was a Lagrangian contact algorithm [Simo and Laursen (1992)] using Surface-to-Surface CONTACT174 and TARGET170 [ANSYS (2002)-b] for the contact and target elements, respectively. The coefficient of friction between the steel frame surface and the masonry wall was taken as 0.6 with zero cohesion between the steel and the wall. In all the models used to verify the modelling approach, the steel frame was modelled exactly as built including the location of the base bolts that resulted in a semi-rigid connection [El-Dakhakhni et al. (2004)]. The top joint stiffeners that prevented premature yielding of the joints under the applied actuator loading and the columns base stiffeners were also include. For the walls, the webs and the face shells were explicitly modelled, however the mortar joints were not. While possible, to explicitly model the mortar joints would have required more than ten times the elements required to model the masonry wall. In addition, to facilitate meshing, the block webs were assumed to be uniformly distributed along the wall while keeping the number of webs in the wall model the same as the actual wall. This was thought to have minimum impact on the wall behaviour, especially since the walls were face shell mortar bedded, not fully bedded. In addition, the contact between the infill wall and the steel frame sections was specified to occur between the steel section flanges and the face shell only, again simulating actual construction of the specimens.

4 Model Verification

The experimental study reported by El-Dakhakhni et al (2004) included **U**nstrengthened **S**olid (no opening) **I**nfill wall, named hereafter **USI**, and an FRP **S**trengthened **S**olid **I**nfill wall, **SSI**. An additional two infill walls had symmetric door openings; again one was **U**nstrengthened **O**pened **I**nfill wall, **UOI**, and the other was FRP **S**trengthened **O**pened **I**nfill wall, **SOI**. For comparison, a bare (without wall) steel frame specimen, **BARE** is also included.

4.1 Specimen BARE

The FE predicted load-deflection values vs. the experimental results for Specimen **BARE** are shown in Fig.2-a. In addition to the observed close agreement, the model also accurately predicted the permanent plastic deformation at the column bases (Fig 2-b) and the formation of the plastic hinge at the beam column connection (Fig 2-c) similar to the experimental observations. It is worth mentioning that the behaviour of the steel material was modelled using a bilinear stress-strain relation with initial Young's modulus of 200 GPa and a tangent modulus of 2 GPa for the post yield region. However, the predicted load-deflection relation is not exactly bilinear. This behaviour corresponds with the test data and was due to the semi-rigid connection at the column bases.

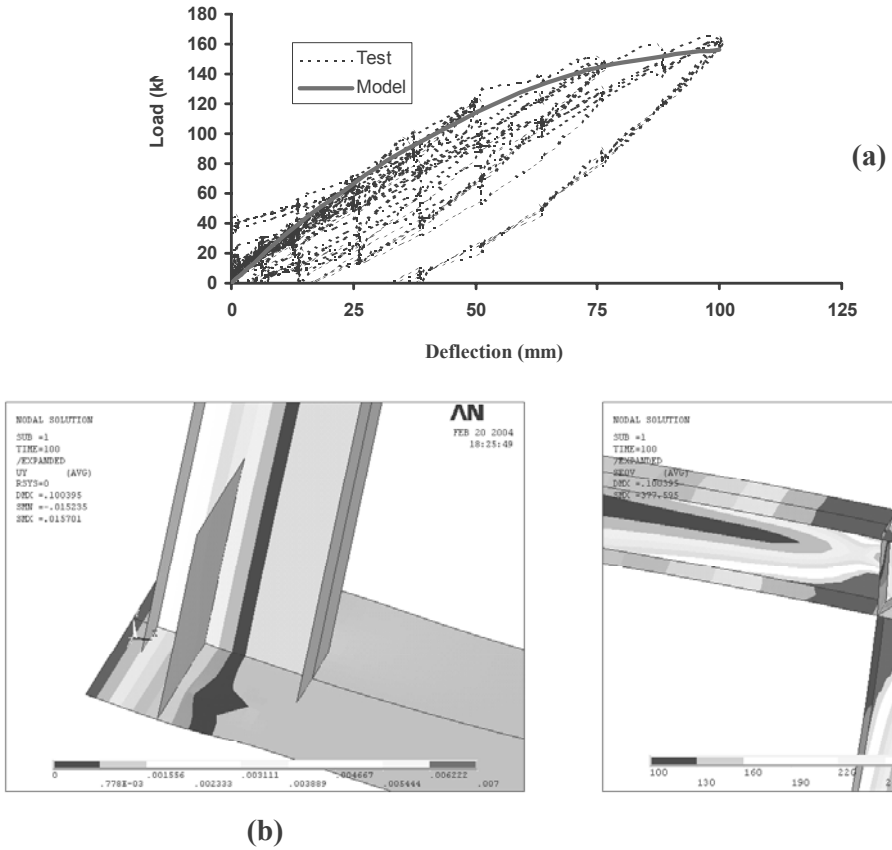

Figure 2 FE Predicted Behaviour for Specimen BARE: a) Load-Deflection Relation, b) Column Base Upward Displacement, and c) Column Top Yielding

4.2 Specimens USI and SSI

The next step to assess the validity of the modelling approach was to model an infilled frame representing Specimen **USI**. The predicted load-deflection behaviour and the experimental values are shown in Fig.3-a. The model accurately predicted the stiffness of Specimen **USI** and its load capacity up to failure. However at the 50 mm deflection level, the test specimen attained a load of 440 kN during the first 50 mm cycle whereas, for the rest of the 50 mm cycles, the specimen had a capacity of 230 kN which was accurately predicted by the model.

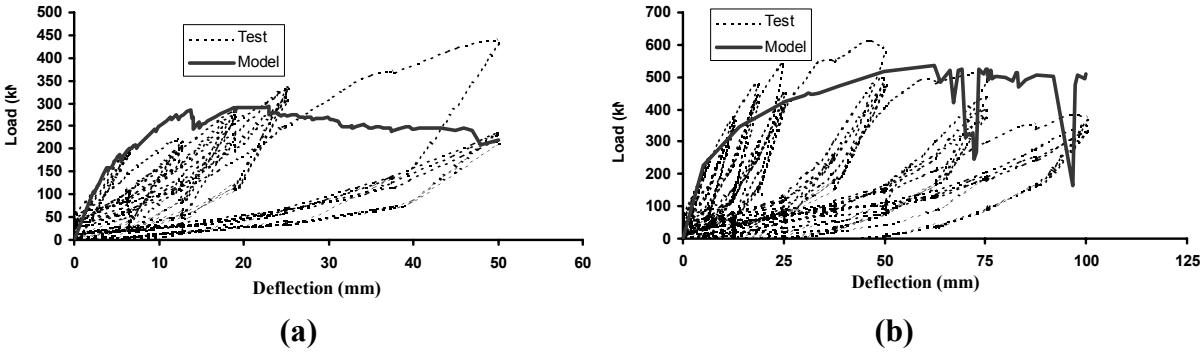

Figure 3 Experimental vs. Predicted Load-Deflection for Specimens: a) USI and b) SSI

Specimen **SSI** was similar to Specimen **USI** except that it had FRP laminate externally adhered to both wall face shells. The FRP was modelled as a membrane only shell

overlaying the masonry face shell elements using four node elastic shell elements, SHELL41 [ANSYS (2002)-b] with orthotropic elastic material behaviour. In addition, since no delamination was observed during testing, all coincident nodes of the masonry face shell and the FRP laminate were coupled using constraint equations specifying the same displacement for each pair of nodes in the two materials. The predicted load-deflection relation and the experimental values are shown in Fig.3-b. The model accurately predicted the stiffness of the Specimen **SSI** and its load capacity up to failure. Similar to the experimental observations, the model predicted yielding of the steel frame column flanges (Fig 4). Yielding resulted from the higher masonry compressive strength (28 MPa) in this specimen compared to the 16 MPa masonry in Specimen **USI**. The transfer of force between the frame and the infill wall was entirely through contact between the face shell of the wall and the flanges of the steel sections. [It is worth mentioning that this local yielding behaviour can only be simulated using a 3-D FE analysis. Currently, this may not be considered in the analysis and design of masonry infilled steel frames where, typically, a macro model is employed by replacing the steel frame members with a 1-D beam-column elements and the masonry wall is modelled as a 1-D equivalent strut.]

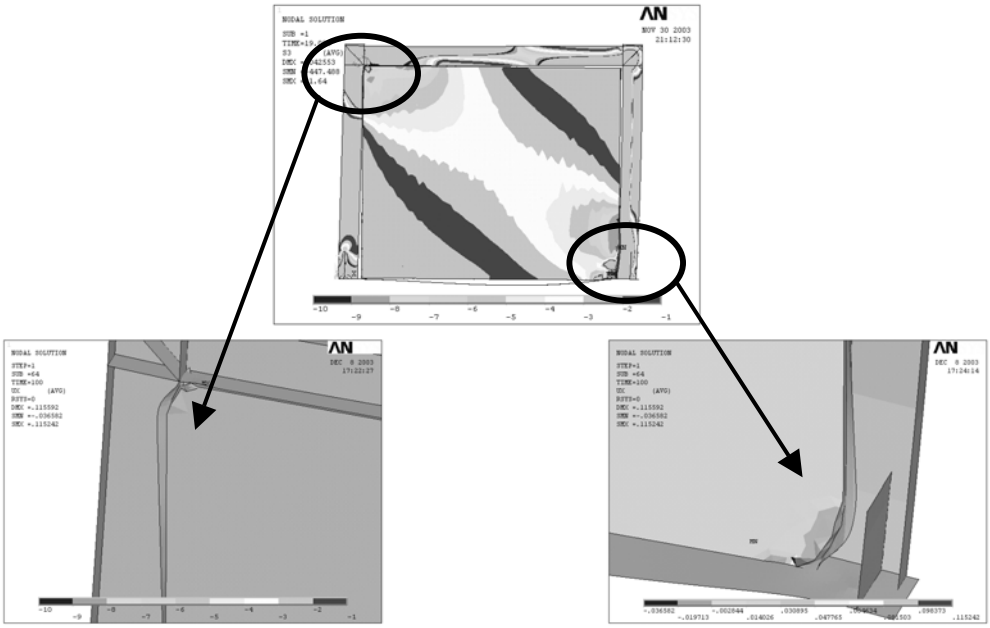

Figure 4 FE Predicted Steel Frame Damage for Specimen SSI

4.3 Specimens UOI and SOI

Figures 5-a and 5-b show the predicted vs. the experimentally obtained load-deflection relations for Specimens **UOI** and **SOI**, respectively. The FE models underestimated the stiffness and the ultimate load of the **UOI** and **SOI** specimens which contained door openings. However, considering the high nonlinearity associated with the models, the results are acceptable. Although it might be expected that wall sections on both sides of the door opening would act as diagonal struts to resist the lateral loads, the FE model showed that only the right side wall formed a strut mechanism when the frame was pushed to the right as shown in Fig. 6. This behaviour resulted from the lack of any lateral restraint at the bottom of the wall on either side of the door opening. Hence, as can be seen in Fig. 6, the left wall section was free to slide along the base while the right wall section was restrained by the right column. The FE model showed that no strut developed on the left side of the opening.

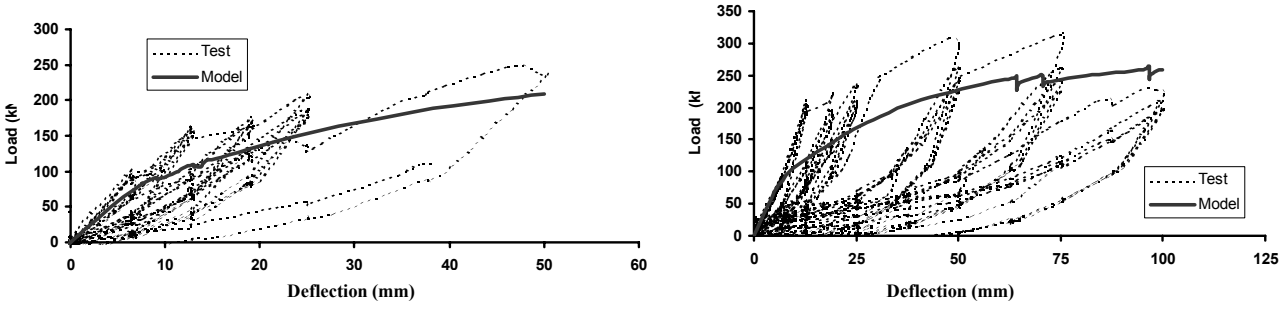

(a) **(b)**

Figure 5 Experimental vs. Predicted Load Deflection for Specimens a) UOI and b) SOI

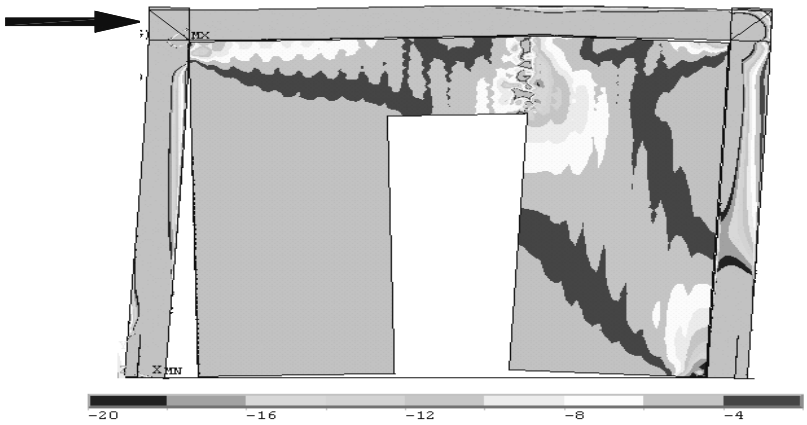

Figure 6 Strut Mechanism Predicted by FE Model for Specimen UOI

5 Parametric Study

5.1 General

The following sections describe the results of a parametric study conducted using the same modelling approach described earlier. In this study, the same steel frame model and specimen geometry as described earlier were used. The parameters studied included masonry strength, boundary conditions and different opening sizes. The effects on stiffness, strength and failure modes as well as the development of strut mechanisms were studied.

5.1.1 Effect of masonry strength

Figure 7-a shows the predicted load-deflection results for four solid masonry infilled steel frames as well as the bare steel frame. The four models had 10, 16, 28 and 40 MPa masonry compressive strengths. The models with 10 and 16 MPa masonry compressive strengths were modelled without FRP strengthening and the models with 28 and 40 MPa masonry were modelled with the same FRP strength. The infilled frame model with the 10 MPa strength exhibited a combined corner crushing and shear failure mode, while the 16 MPa model exhibited only corner crushing failure. Neither model predicted any damage to the steel frame flanges unlike the models with 28 MPa and 40 MPa masonry walls that predicted significant damage to the steel flanges with minor corner crushing within the walls. Figure 7-b shows the lateral displacement of the 10 MPa wall model which predicted shear failure at approximately the wall midheight. Figures 7-c, 7-d and 7-e show the changes in the principal compressive stresses with

increasing top deflection of 9.8,18.9 and 72.9 mm, respectively for the 10 MPa wall model. As can be seen in the figure, at 9.8 mm the wall acted as a single diagonal strut connecting the left top beam-column connection to the opposite column base. At approximately 12 mm, the wall started to develop a secondary strut connecting the left top beam-column connection to the middle of the opposite column. This behaviour continued with increased top deflection (see Fig. 7-d) until the original main strut started to deteriorate at approximately 73 mm as seen in Fig. 7-e. This may indicate the start of a *knee brace* behaviour as explained by Paulay and Priestley (1992).

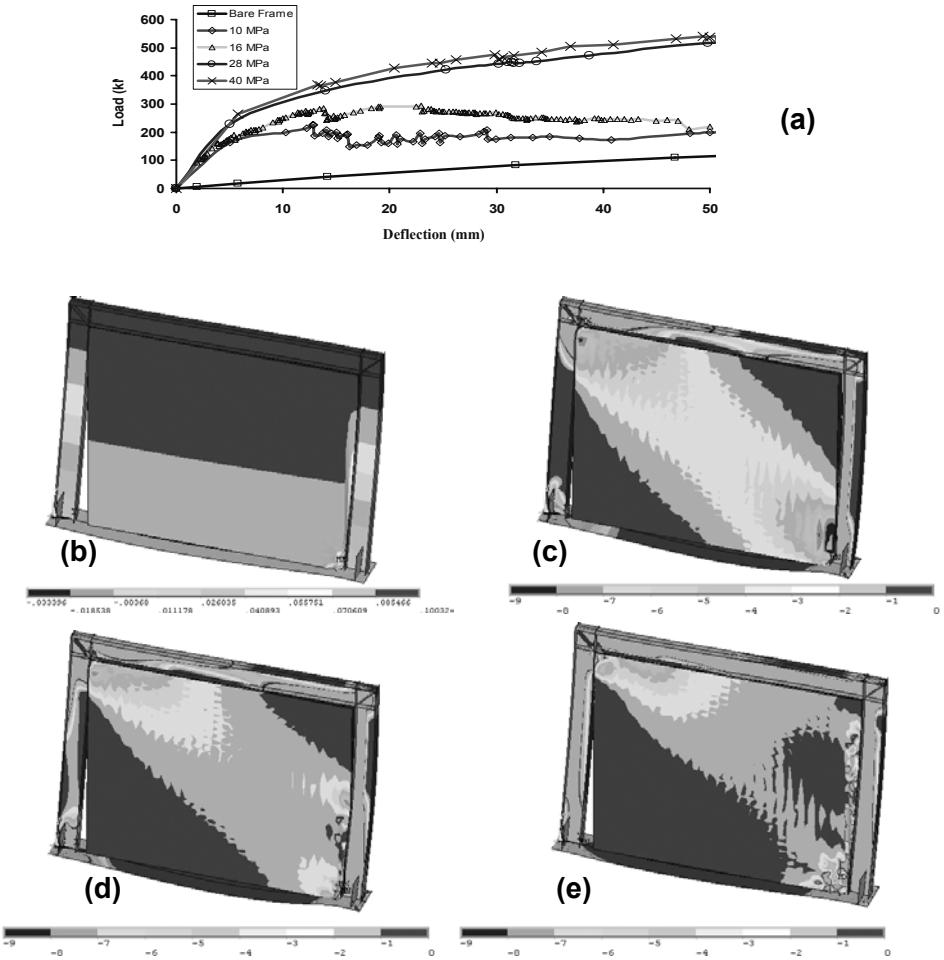

Figure 7 Solid Infill Models: a) Effect of Different Masonry Strengths; and for the 10 MPa Model: b) Lateral Deflections, c) Principal Compressive Stresses at 9.8 mm Deflection, d) Principal Compressive Stresses at 18.9 mm Deflection and e) Principal Compressive Stresses at 72.9 mm Deflection

5.1.2 Effect of steel angle at door opening

In order to force the wall section on the left side of the door opening in Specimen **SOI** to engage in resisting the lateral load, a 200x200x20 mm steel angle was placed at each of the two lower corners of the opening. It was thought that this angle would provide enough resistance to lateral movement for the left wall section to form a diagonal strut. As can be seen from Fig. 8-a, a secondary diagonal strut was indeed formed within the left wall section and resulted in significant stiffness and strength increases as can be seen in Fig. 8-c. The relative benefit of this secondary strut decreased at higher deflections as a result of yielding of the steel angle (see Fig. 8-b).

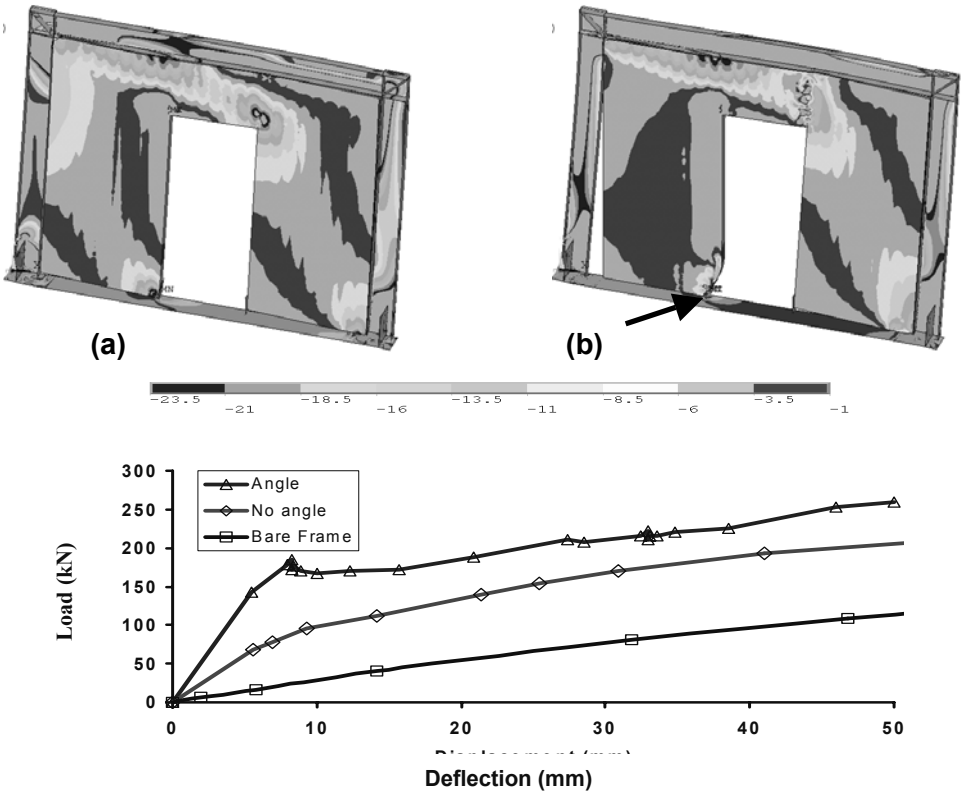

Figure 8 Effect of Steel Angle at the Door Toe: a) Formation of the Strut in the Left Wall Section, b) Yielding of Steel Angle and c) Load-Deflection Behaviour

5.1.3 Effect of window openings

To assess the effect of a symmetrical window opening, two window sizes were chosen, namely 1.0x1.0 m and 1.8x1.8 m, representing 10 % and 34 % of the wall area, respectively. The strut mechanisms formed around these two windows are quite different as can be seen in Figs. 9-a and 9-b. In addition, the strengths and stiffnesses are also quite different as can be seen in Fig. 9-e. However, similar to the model with the door opening and steel angles, the models with window openings formed two distinct strut mechanisms. The main mechanism connected the left top beam-column connection to the opposite column by passing through the part of the wall on top of the opening and then diagonally down the right wall to the lower part of the column. The secondary (less stressed) strut mechanism passed through the left part of the wall and into the part of the wall under the window. It is important to note the effect of these strut mechanisms on the steel frame. The top (main) strut formed in the small window model resulted in yielding of the steel column at around 35% of its height as can be seen in Fig. 9-c. On the other hand, bearing against the top beam by the main strut formed over the opening in the large window model resulted in a point of maximum moment at approximately 80% of the beam span measured from the left column. Figure 9-d shows the vertical deflection contours for a lateral displacement of 50 mm, where the upward deflection of the top beam was caused by the strut action. From the load-deflection results in Fig. 9-e, it can be seen that the small and the large window models resulted in reduction of initial stiffness of 76% and 36%, respectively. Models from other studies for similar opening percentages estimated 68% and 25% reduction [Giannakas et al. (1987)] and 82% and 42% reduction [Mosallam et al. (1997)] for the small and the large window, respectively.

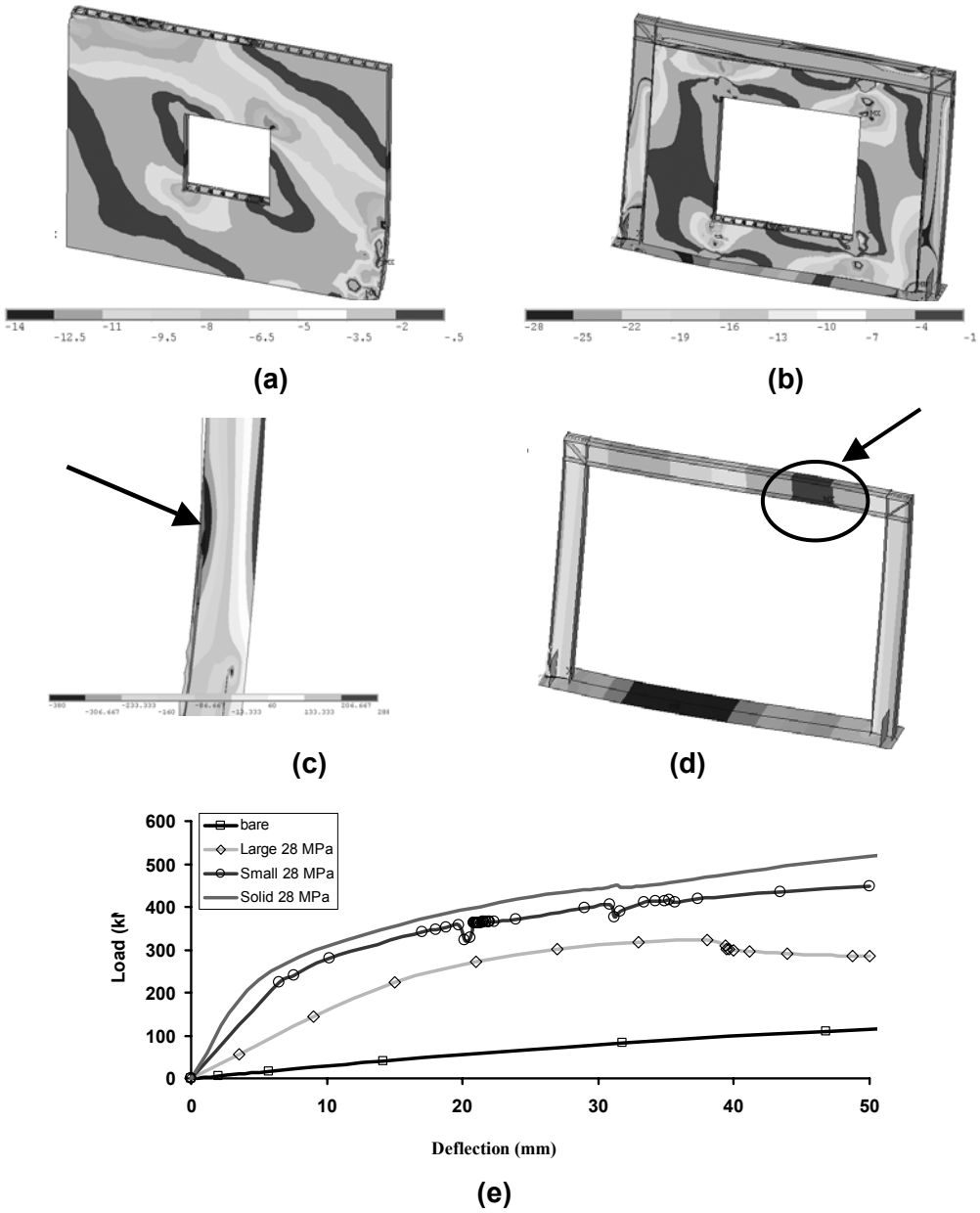

Figure 9 Effect of Window Opening: a) Principal Compressive Stresses in the Small Window Model, b) Principal Compressive Stresses in the Large Window Model, c) Yielding of the Steel Column of the Small Window Model, d) Point of Maximum Deflection in the Beam of the Large Window Model, e) Load-Deflection Behaviour

6 Conclusions

The following conclusions can be drawn from the study:

1. The modelling technique was shown to serve as a useful computational tool to gain insight on possible strut mechanisms within infill walls including walls with openings. This type of analysis will enable design engineers to locate critical sections within the surrounding frame that might not be that critical without the infill wall. Local yielding effects are also identified.

2. Even though the modelling technique did not directly predict the observed cracking, the failure criterion captures loss of strength and stiffness associated with material failure to produce nearly the same behaviour.

3. Infill walls within frame structures dramatically change the stiffness, strength and post-peak behaviour. In order to accurately predict the behaviour of infilled frames, the nonlinearities associated with the different constituent materials and the contact problem must be accounted for. In addition, accurate geometrical representation is required.

4. The higher strengths and, very importantly, stiffnesses predicted for the infilled frame models compared to the bare frame shows the importance of including the infill wall effects in the analysis and design of infilled frame structures.

Acknowledgement

This study forms a part of ongoing research in The McMaster Centre for Effective Design of Structures funded through the Ontario Research and Development Challenge Fund.

References

ANSYS Theory Manual, (2002-a), Release 6.1, ANSYS Inc., Canonsburg, USA

ANSYS Element Manual, (2002-b), Release 6.1, ANSYS Inc., Canonsburg, USA

Comite Euro-International Du Beton (1996) “RC Frames Under Earthquake Loading”, Thomas Telford Services Ltd., London, UK

El-Dakhakhni, W.W., Hamid, A.A. and Elgaaly, M. “Seismic Retrofit of Concrete-Masonry-Infilled Steel Frames using GFRP Laminates” (In-press) to be published in 2004 ASCE Journal of Structural Engineering

Giannakas, A., Patronis, D., and Fardis, M. (1987) “The Influence of the Position and Size of Openings to the Elastic Rigidity of Infill Walls”, Proc., 8th Hellenic Concrete Conf. Xanthi, Kavala, Greece, 49-56.

Mosalam, K. M., White, R. N. and Gergely, P. (1997) “Computational Strategies for Frames with Infill Walls: Discrete and Smeared Crack Analyses and Seismic Fagility,” Technical Report NCEER-97-0021, Buffalo, New York.

Paulay, T. and Priestley, M. J. N. (1992) “Seismic Design of Reinforced Concrete and Masonry Buildings,” John Wiley & Sons, Inc., New York, NY, USA.

Simo, J.C. and Laursen, T.A., "An Augmented Lagrangian Treatment of Contact Problems Involving Friction", Computers and Structures, Vol. 42, No. 1, pp. 97-116 (1992).